East European Journal of Physics. 1. 406-412 (2026)
DOI:10.26565/2312-4334-2026-1-49 ISSN 2312-4334

STOPPING POWERS AND CSDA RANGE FOR POSITRON AND ELECTRON IN HUMAN KIDNEY, LUNG AND THYROID ORGANS

Hawar M. Dlshad[1]*, Jamal M. Rashid[2]
[1]*University of Sulaimani, college of Education, department of Physics, Sulaymaniyah 46001, Kurdistan Region, Iraq*
[2]*University of Sulaimani, college of science, department of Physics, Qlyasan street, Sulaymaniyah 46001, Kurdistan Region, Iraq*
**Corresponding Author E-mail: Hawar.dlshad@univsul.edu.iq*
Received October 9, 2025; revised January 23, 2026; accepted February 2, 2026

This study computed the stopping power of positrons in a few biological tissues in the energy range of 100 eV to 1 MeV. The base of the method is using the modified Bethe-Bloch expression for stopping power and effective atomic number analytical expression including key parameters such as the mean excitation energies of the target atoms that significantly impact stopping power results. Analytical formulas were mostly used to calculate the stopping power and continuous slowing down approximation CSDA range. The calculated results of the stopping power and range for positrons in a few compounds, such as kidney, lung and thyroid tissue are compared with other calculation results like Penelope 2012 program. Monte Carlo simulation was used for the calculations. The results were plotted in graphs to show the contrasts. And they satisfy a recognized need in the medical physics community for tissue-specific positron interaction data, with immediate applications in improving positron emission tomography (PET) image quantification accuracy and refining radiation dose for β^+emitting radiopharmaceuticals.
Keywords: *Stopping power; Positron; CSDA range; Excitation energy; Human tissue*
PACS: 34.85.+x, 34.50.Bw, 78.70.Bj, 87.15.-v, 34.80.Gs

1. INTRODUCTION

The positron, the antiparticle of the electron, can be used in many medical fields. Most notably, they find application in particle physics and medical imaging, particularly in positron emission tomography (PET) and Gamma knife radiotherapy [1]. Also, they can be used as therapies for cancer [2]. Over the last three decades, positrons have shown to be a useful probe for examining both vacancy type bulk defects and metal electronic structure especially for polymers [3]. It is also used in other fields such as chemistry, radiation physics, particle physics, biology, and nuclear medicine, stopping power (SP) is crucial.

On the other hand, stopping power (SP) is an energy loss process that decelerates highly charged particles moving through matter. It includes complex scattering interactions between the incident charged particle and electrons and nuclei of the atoms [4].

The calculations of positron SP have received less attention than calculations of electrons, despite the fact that positron and electron paths in matter are typically considered to be similar in which there is a little difference [2]. Numerous researchers have examined SP calculations for positrons and electrons [5], both theoretically and practically [6]. Pal discussed the Wilson theory, where it led to the development of new straightforward empirical formulas for the electrons and positrons total mass SP in material [7]. In absorbers with atomic numbers ranging from Z = 1 to 92, the formulas hold true in the energy range between 5 Mev and 1000 MeV for electrons and positrons. Furthermore, Batra [8] has explored the total mass SP equations for low energy positrons from 1 KeV to 500 KeV in absorbers in terms of energy parameters. Some particles have approximate SPs that match the latest theoretical predictions. The investigated SPs are compared with available data. Moreover, Hasan Gümüş has created a new algorithm for calculating SP for incoming positrons [9]. A modified formula of Rohrlich and Carlson SP for positron intermediate energies is considered. The statistical atomic density models provided by Lenz and Jensen have been used in calculations. They had calculated the SP of some materials for positrons like aluminum, silicon, copper and liquid water. Additionally, they determined the SP formulas for positrons using the generalized oscillator strength model. The SP of several biological compounds and targets with low atomic numbers for positrons were computed for energies ranging from 50 eV to 10 MeV [10]. In a number of water-equivalent polymer gel dosimeters, Hikmet Osman et al. [11] have investigated SP and the continuous slowing down approximation (CSDA) range for electrons and positrons within the level of energy between 20 eV and 1 GeV.

This work aims to determine the stopping power and CSDA range for positrons and electrons. The Rohrlich and Carlson which is a special type of modified Bethe-Bloch formula used as analytical method. Some biological compounds like: kidney, lung, and thyroid are used in the study which can be valid for all energy regions from low to intermediate and reach high energies positions (relativistic energies). The comparison made between the obtained results and the theoretical results found by the Penelope 2012 program due to lack of the experimental data. Finally, the results have been graphed for better visual understanding.

Cite as: H.M. Dlshad, J.M. Rashid, East Eur. J. Phys. 1, 406 (2026), https://doi.org/10.26565/2312-4334-2026-1-49

2. METHODOLOGY

2.1 Stopping Power calculations

The stopping power of positrons divided in to two parts: The first is collision stopping power, which takes into account the electromagnetic interactions of arriving positrons with the bound electrons of the target. The second is to take into account the emission of photons, also known as radiative stopping power or Bremsstrahlung radiation, that occurs when positrons accelerate within the electromagnetic fields of target nuclei. The total mass stopping power is given as follows [6]:

$$S_{Total}(E) = S_{coll}(E) + S_{rad}(E) \tag{1}$$

In this article, modified Bethe-Bloch formula is chosen to calculate the total mass SP [12]. Since our analysis focuses on the low and intermediate energy range, the radiative SP can be disregarded due to its negligible contribution at these energy levels. However, the Penelope simulation incorporates both collision and radiative stopping power components in its computational framework, regardless of energy range. This methodological difference represents a key distinction between our analytical approach and the Monte Carlo simulation. While Bethe and Heitler exclude the radiative term based on its minimal impact at lower energies [13].

$$S_{rad} = S_{coll}^{\pm}\left(\frac{Z\,E}{800}\right), \tag{2}$$

where S_{rad}, S_{coll} are the radiation, and collision stopping power. The superscripts (+) and (-) stand for positrons and electrons, respectively. Z, E are the target atomic number, and the incident energy of positrons or electrons in unit of MeV. Therefore, the total mass stopping power represents by collision stopping power only (Rohrlich and Carlson) [12] as follow:

$$\frac{1}{\rho}S_{coll} = \frac{2\pi N_a r_e^2 m c^2}{\beta^2}\frac{Z_{eff}}{A}\left[\ln\left(\frac{T}{I}\right)^2 + \ln\left(1+\frac{T}{2}\right) + F^{+}(\tau) - \delta\right]. \tag{3}$$

Here, ρ is the medium density ($\mathrm{gm/cm^3}$), r_e is the classical radius of electron which is equal to (2.8179×10^{-15}meters), mc^2 is the electron rest energy (0.5110034 MeV), T is the incident particle energy, $F^{\mp}$ is a function defined later for electron and positron, and Z_{eff} is effective atomic number of the target taken from Markowicz-Van Grieken expression and given by [14, 15]

$$Z_{eff} = \frac{\sum_{i=1}^{l}\frac{w_i Z_i^2}{A_i}}{\sum_{i=1}^{l}\frac{w_i Z_i}{A_i}}, \beta^2 = 1 - \frac{1}{\left(1+\frac{T}{mc^2}\right)^2} \tag{4}$$

Where w_i represents the weight fraction of each constituent element, Z_i and A_i are atomic and mass number of i element in the biological compound target respectively. Additionally, the value of β^2 is not taken from other references like: Seltzer and Berger work [16]. It calculated for all amount of energy with the above equation.

Similarly, the effective mean excitation energy of the medium (I), which is defined as the average energy required to excite electrons in the target material, is calculated by using logarithmic averaging methods such as Bragg's elemental additivity rule [15]:

$$\ln I = \frac{\langle\frac{Z}{A}\rangle \ln(I_i)}{\langle\frac{Z}{A}\rangle}, and\ \langle Z/A\rangle = \sum_i w_i\left(\frac{Z_i}{A_i}\right) \tag{5}$$

Here, I_i is the corresponding elemental mean excitation energy. For biological tissues, this calculation is particularly complex due to the heterogeneous nature of organic compounds and the presence of hydrogen bonding, which can significantly modify electronic properties. Cohen and Taylor Used for the numerical values [17] for the various physical constants for both positron and electron, one finds that:

$$F^{+}(\tau) = 2\ln 2 - \frac{\beta^2}{12}\left[23 + \frac{14}{(\tau+2)} + \frac{10}{(\tau+2)^2} + \frac{4}{(\tau+2)^3}\right], \tag{6}$$

And for electron as:

$$F^{-}(\tau) = 1 - \beta^2\left[1 + \frac{\tau^2}{8} - (2\tau+1)\,ln2\right]. \tag{7}$$

Where $\tau = T/mc^2$ is the ratio between the kinetic energy of the incident particle and its rest energy, δ density-effect correction is equal to [16]:

$$\delta = 2\ln\left(\frac{\hbar\omega}{I}\right) + 2\ln(\tau+1) - 1 \tag{8}$$

Where $\hbar\,\omega = 28.816\,(\frac{\rho Z}{A})^{1/2}$ is the plasma energy in eV, the quantity of (δ) too small at low energies, therefore, we can neglect it in our calculations.

2.2 CSDA Range calculations

The charged particle loses energy as it moves through the stopping medium and eventually comes to a stop. The range of the incident charged particle is the distance between the medium's surface, where the incident particle enters, and the incident particle's final location within the medium. And depends on the density of the target. CSDA (Continuous Slowing Down Approximation) Range for incident particles with kinetic energies E_0 is calculated by integrating the reciprocal of the stopping power over energy [6]:

$$CSDA\ (g/cm^2\ ) = \int_{E_f}^{E_0} \frac{dE}{S_{tot}(E)}\ . \tag{9}$$

Where S_{tot} is the total stopping power of the medium, (E_0, E_f) is the initial energy and final energy of it, respectively. If the stopping power chose in $(MeV.cm^2/g)$ units and energy in (eV), one can find, the CSDA range in units of g/cm^2.

3. RESULTS AND DISCUSSIONS

Studies dedicated to positron stopping power calculations have received substantially less scholarly attention than their electron, with many analyses conventionally assuming positron behavior in matter closely resembles that of electrons despite their antimatter nature. However, this approximation requires careful validation across different energy ranges and materials. When determining positron or electron SPs with precision, our methodology first needs to calculate the effective charge of target materials by using Eq. (3), which accounts for the composite electronic structure of compound like biological tissues. Simultaneously, we derive the mean excitation energy with Eq. (5). This foundational step is crucial as it accounts for the unique interaction mechanisms between positron or electron and target materials. Unlike electrons, positrons exhibit different scattering behaviors due to their positive charge, which creates repulsive interactions with nuclei rather than attractive ones. Then these values have been used in Eq. (3) to calculate total mass stopping power of the medium for positrons. Moreover, the CSDA range of a particle moving through the cell thickness depends on the excess energy of the particle. We applied our method to some tissues like: kidney, lung and thyroid targets because they have wide applications in the area of Nuclear Medicine. The composition of materials for each kidney, lung, and thyroid tabulated in Tables (1).

Table 1 Material composition of Kidney, Lung, and Thyroid [18-20]

Fraction by weight			
Element	**Kidney**	**Lung**	**Thyroid**
H	0.103	0.103	0.104
C	0.132	0.105	0.119
N	0.030	0.031	0.024
O	0.724	0.748	0.745
Na	0.002	0.002	0.002
P	0.002	0.002	0.001
S	0.002	0.003	0.001
Cl	0.002	0.003	0.002
K	0.002	0.002	0.001
Ca	0.001	-	-
I	-	-	0.001
Density ρ (g/cm^3)	1.04	0.25	1.05

The core and valence electron excitation energies were calculated for the elemental composition of kidney, lung, and thyroid tissues. These values were applied within Gryzinski's excitation function to determine the total ionization cross-section for inelastic scattering [21]. Subsequently, the derived cross-sections were used to compute the mean excitation energy for each biological material. The fundamental data for the compound elements are provided in (Table 2).

Table 2 Atomic number, atomic mass, and excitation energy of elemental composition of the three compounds [20]

Atoms	**Atomic number (Z)**	**Atomic mass (A)**	**Calculated**	
			I_{core} (eV)	**$I_{Valence}$ (eV)**
H	1	1.00784	-	-
C	6	12.011	19.320	11.70
N	7	14.0067	25.85	15.51
O	8	15.999	33.742	17.143
Na	11	22.989769	41.361	4.898
P	15	30.973762	19.047	10.612
S	16	32.065	23.946	11.973
Cl	17	35.453	29.116	13.877

Atoms	Atomic number (Z)	Atomic mass (A)	Calculated	
			I_{core} (eV)	$I_{Valence}$ (eV)
K	19	39.0983	25.850	4.081
I	53	126.90447	22.313	10.884
Mg	12	24.312	62.041	6.802
Ca	20	40.078	36.463	5.442

Now, the calculation results of this work on SPs and CSDA ranges as a function of incident positron or electron energy for each compound are shown graphically in Figures (1-6). In all figures the red dashed line represents our work results for positron, the blue solid line Penelope 2012 results, and the green lines represent this work SPs for electron.

Fig. 1 illustrates the total SP for kidney, it expressed in units of (MeV·cm²/g), for incident positron and electron energies ranging from 100 eV to 1 MeV. The result of calculations are compared with those obtained from the Penelope 2012 program (Monte Carlo code). Generally, there is a good agreement between them along the whole energy ranges, although some discrepancies are observed at lower energies. The disagreement between the three methodologies ranges from approximately 20-30% at lower energies, decreasing gradually to about 10-15% at energies exceeding 100,000 eV. And Fig. 2 presents the CSDA range in the kidney as a function of positron or electron energy. The two quantities exhibit a direct proportional relationship. The figure demonstrates a gradually increasing slope, indicating that the rate of increase in CSDA range becomes greater at higher energies. And the similarity between positron and electron results are high although does not appear in plot but there are some differenet especialy in the energy range of 5 KeV to 10 KeV. This non-linear behavior reflects the complex physics of interactions of positron and electron with matter.

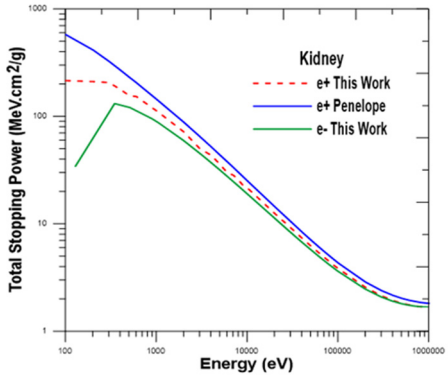

Figure 1. Total mass stopping power for incident positron, electron energies in Kidney. The results of this work and Penelope 2012

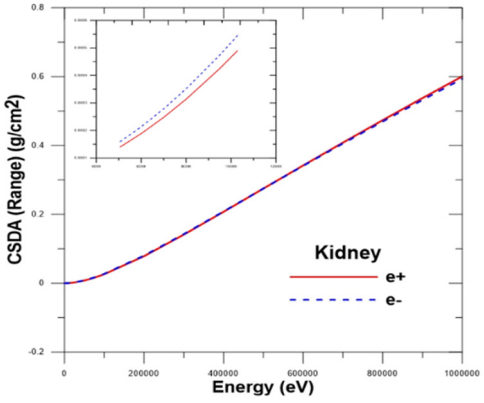

Figure 2. CSDA Range of positron, electron in Kidney

Fig. 3 shows that the calculated results generally agree well with those from the Penelope simulation; however, some disagreements are observed in the low-energy region under 1 keV. The graph demonstrates that three results of SP decrease with increasing the positron energy. The curve appears to converge somewhat at the highest energies (1 MeV), indicating better agreement between methods as relativistic effects become more dominant and quantum-mechanical corrections less significant.

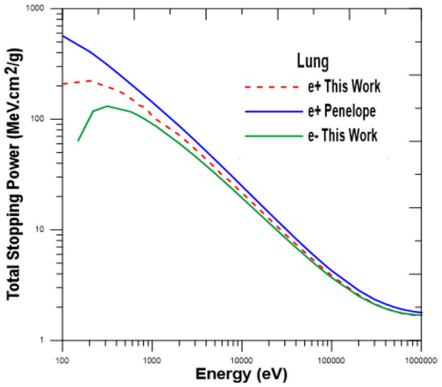

Figure 3. Total mass stopping power for incident positron, electron energies in Lung. The results of this work and Penelope 2012

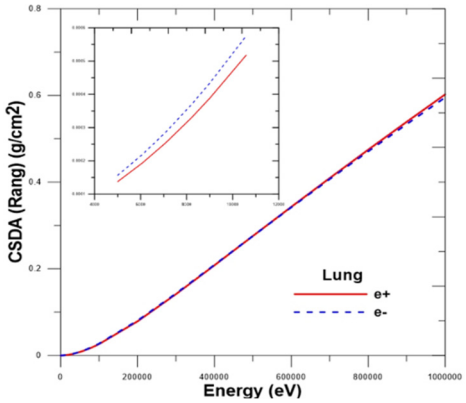

Figure 4. CSDA Range of positron, electron in Lung

The differential between the two techniques amounts to about 20-30% in the low-energy region, systematically reducing to around 10-15% at energies beyond 100,000 eV. Fig. 4 illustrates the relationship between the CSDA range and positron and electron energies. The graph demonstrates a clear non-linear relationship between each positron and electron energy and range. As the energy increases, the CSDA range increases at an accelerating rate, particularly at higher energies. This follows the expected physics, where higher-energy particle penetrates deeper into tissue. Moreover, for 1 MeV positrons

in lung tissue, the CSDA range reaches approximately 0.46 g/cm². This represents the maximum penetration depth, which is particularly relevant for medical applications such as PET imaging and radiation therapy planning.

In Fig. 5, our work analytical calculations constantly predict higher SP values than the Penelope simulations across the entire energy range.

This difference is most pronounced at lower energies (100-1000 eV) and gradually narrows at higher energies due to the different compositions and densities of tissues, which affect how positrons and electrons lose energy as they travel through them. The unique composition of thyroid makes its stopping power behavior fundamentally different from other tissues, particularly in the low-energy where atomic-level details matter most. These differences including the high density of thyroid compared to kidney and lung as shown in (Table 1). Lower density means fewer interactions per unit path length, resulting in lower stopping power. Moreover, thyroid has higher iodine content (high Z), which significantly affects stopping power.

On the other hand, both methodologies show the expected inverse relationship between SP and positron and electron energy - as the energy increases, SP decreases. This is due to the fundamental principle that higher-energy positrons interact less efficiently with the electron of the medium. The discrepancy between the two approaches is approximately 20-30% at lower energies, reducing step by step to about 10-15% at energies above 100,000 eV. This suggests that theoretical assumptions or correction factors implemented in the analytical approach may differ from those in the MC simulation, particularly in handling low-energy interactions. Fig. 6 the graph exhibits a non-linear relationship between positron and electron energies and range in thyroid tissue. At 1 MeV. Despite some difference between positron and electron result, in the maximum energies the CSDA range reaches approximately 0.47 g/cm². This follows the theoretical expectation that higher-energy positrons or electrons will penetrate deeper into tissue before stopping.

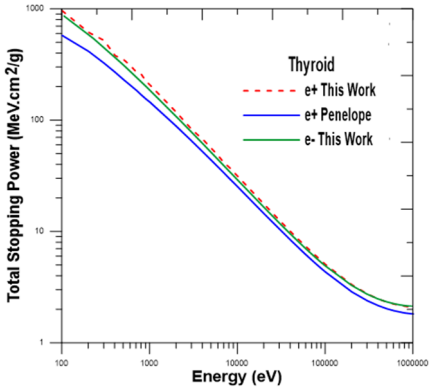

Figure 5. Total mass stopping power for incident positron, electron energies in Thyroid. The results of this work and Penelope 2012

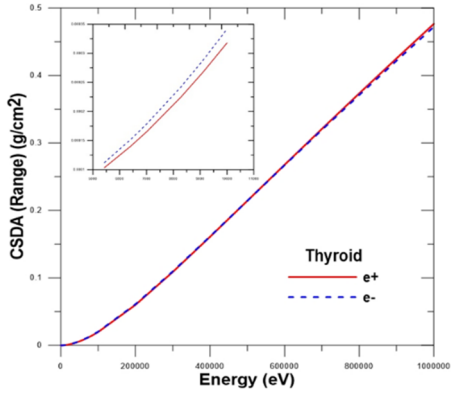

Figure 6. CSDA Range of positron, electron in Thyroid

Equations (6) and (7) define the functions $F^{\pm}(\tau)$ that characterize how collision losses differ between positrons and electrons. These functions, which depend only on the incident energy and are independent of the atomic number, are plotted in Fig. 7. When positrons undergo collisions that loss more than half of their energy, they contribute approximately 0.4 to F^{+}, a value that stays relatively unchanged.

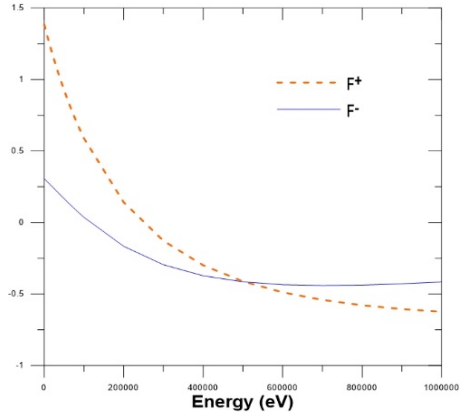

Figure 7. The functions $F^{+}(\tau)$ and $F^{-}(\tau)$, which occur in the average energy loss formulas for both positrons and electrons, as function of Energy in (eV)

4. CONCLUSIONS

The SP have been studied for several biological compounds like: Kidney, Lung, and thyroid. Positron and electron are used as a projectile particle with a range of energy between (100 eV to 1.0 MeV). The model that used in this work is the modified Bethe Bloch formula. The methodology employed in this study offers significant computational advantages

through analytical approach to SP determination. By including targeted parameter adjustments that account for compound-specific characteristics, we transform complex SP calculations into a straightforward mathematical framework accessible without extensive computational resources. The relationship between SP and positron and electron energies demonstrate an inverse correlation as energy increases, SP correspondingly decreases.

Additionally, this analytical framework extends naturally to Continuous Slowing Down Approximation (CSDA) range calculations, enabling rapid determination of positron and electron penetration depths in various biological media. Only our analytical calculations are presented for relation between CSDA range and positron and electron energy without comparison to other methodologies or experimental data because there are no any previous work and references. This makes it difficult to assess the accuracy of these specific calculations. We denote that, the curves appear remarkably similar in shape and magnitude. Despite the different tissue compositions and densities between kidney, lung and thyroid. Although the results of both positron and electron are appeared to be exactly the same but in the energy range between 5 KeV to 10 KeV they have differences as shown in zoomed plot. Finally, our future work should focus on experimental approve to confirm these calculations and extension to additional biological tissues and composite materials of medical significance.

Declaration of competing interest

The authors declare that they have no known competing financial interests or personal relationships that could have appeared to influence the work reported in this paper.

ORCID

Hawar M. Dlshad, https://orcid.org/0000-0002-6430-8106

REFERENCES

[1] S.N. Ahmed, "Properties and sources of radiation," Physics and Engineering of Radiation Detection, 1–64 (2015). https://doi.org/10.1016/B978-0-12-801363-2.00001-2

[2] M.E. Juweid, and B.D. Cheson, "Positron-Emission Tomography and Assessment of Cancer Therapy," N. Engl. J. Med. (354), 496–507 (2006). https://doi.org/10.1056/NEJMra050276

[3] K.G. Lynn, and H. Lutz, "Slow positrons in single-crystal samples of Al and Al-Al_xO_y," Phys Rev B, **22**(9), 4143–4160 (1980). https://doi.org/10.1103/PhysRevB.22.4143

[4] M.K. Saadi, and R. Machrafi, "Development of a new code for stopping power and CSDA range calculation of incident charged particles, part A: Electron and positron," Applied Radiation and Isotopes, **161**, (2020). https://doi.org/10.1016/j.apradiso.2020.109145

[5] L. Cai, "Monte Carlo simulation of positron induced secondary electrons in thin carbon foils," The University of Hong Kong, Pokfulam Road, Hong Kong SAR, 2010. https://doi.org/10.5353/th_b4546086

[6] M. Ç. Tufan, and H. Gümüş, "A study on the calculation of stopping power and CSDA Range for incident positrons," Journal of Nuclear Materials, **412**(3), 308–314 (2011), https://doi.org/10.1016/j.jnucmat.2011.03.016

[7] P.B. Pal, V.P. Varshney, and D.K. Gupta, "Total stopping power formulae for high energy electrons and positrons," Nucl. Instrum. Methods Phys. Res. B, **16**(1), 1–4 (1986). https://doi.org/10.1016/0168-583X(86)90220-X

[8] R.K. Batra, "Approximate stopping power of low energy electrons and positrons in matter," Nucl. Instrum. Methods Phys. Res. B, **28**(2), 195–198 (1987). https://doi.org/10.1016/0168-583X(87)90104-2

[9] H. Gümüş, O. Kabaday, and A.G. Tufan, "Calculation of the Stopping Power for Intermediate Energy Positrons," Chinese Journal of Physics, **44**(4), (2006). [Online]. http://PSROC.phys.ntu.edu.tw/cjp

[10] H. Gumus, T. Namdar, and A. Bentabet, "Positron stopping power in some biological compounds for intermediate energies with generalized oscillator strength model," International Journal of Molecular Biology, **3**(3), (2018). https://doi.org/10.15406/ijmboa.2018.03.00057

[11] H. Osman, and H. Gümüş, "Stopping power and CSDA range calculations of electrons and positrons over the 20 eV–1 GeV energy range in some water equivalent polymer gel dosimeters," Applied Radiation and Isotopes, **179**, 110024 (2022). https://doi.org/10.1016/J.APRADISO.2021.110024

[12] M.J. Berger, and S.M. Seltzer, *Stopping powers and ranges of electrons and positrons*, 2nd ed. (Gaithersburg, MD, 1983). https://doi.org/10.6028/NBS.IR.82-2550A

[13] P.B. Pal, V.P. Varshney, and D.K. Gupta, "Semiempirical stopping power equation for positrons," J. Appl. Phys. **60**(1), 461–463 (1986). https://doi.org/10.1063/1.337623

[14] M.V. Manjunatha, B.M. Sankarshan, and T.K. Umesh, "New method to determine effective atomic number of samples via external bremsstrahlung," X-Ray Spectrometry, **43**(4), 246–252 (2014). https://doi.org/10.1002/xrs.2546

[15] V. De Smet, R. Labarbe, F. Vander Stappen, B. Macq, and E. Sterpin, "Reassessment of stopping power ratio uncertainties caused by mean excitation energies using a water-based formalism," Med. Phys. **45**(7), 3361–3370 (2018). https://doi.org/10.1002/mp.12949

[16] S.M. Seltzer, and M.J. Berger, "Evaluation of the collision stopping power of elements and compounds for electrons and positrons," Int. J. Appl. Radiat. Isot. **33**(11), 1189–1218 (1982). https://doi.org/10.1016/0020-708X(82)90244-7

[17] E.R. Cohen, and B.N. Taylor, "The 1973 Least-Squares Adjustment of the Fundamental Constants*," J. Phys. D: Appl. Phys. **5**, 43–58 (1973). https://doi.org/10.1063/1.3253130

[18] Arectout, *et al.*, "Investigation of photon interaction parameters in Human Body Tissues using GAMOS, FLUKA, and XCOM Studies," Nuclear Analysis, **4**(1), 1–11 (2025). https://doi.org/10.1016/j.nucana.2024.100141

[19] ICRU, "Tissue substitutes in radiation dosimetry ana measurement ICRU report 44," (Bethesda, 1989).

[20] C. Cao, R.E. Vernon, W.H.E. Schwarz, and J. Li, "Understanding Periodic and Non-periodic Chemistry in Periodic Tables," Front. Chem. **8**, (2021). https://doi.org/10.3389/fchem.2020.00813

[21] H.M. Dlshad, and J.M. Rashid, "Monte Carlo code for calculating the elastic and inelastic scattering cross section along with mean free path of positron scattering in kidney, lung and thyroid organs," East Eur. J. Phys, (4), 82-289 (2025). https://doi.org/10.26565/2312-4334-2025-4-61

ГАЛЬМІВНА ЗДАТНІСТЬ ТА ДІАПАЗОН CSDA ДЛЯ ПОЗИТРОНІВ ТА ЕЛЕКТРОНІВ В ОРГАНАХ НИРОК, ЛЕГЕНЬ ТА ЩИТОВИДНОЇ ЗАЛОЗИ ЛЮДИНИ

Хавар М. Длшад[1], Джамал М. Рашид[2]

[1]*Університет Сулеймані, коледж освіти, кафедра фізики, Сулейманія 46001, Регіон Курдистан, Ірак*

[2]*Університет Сулеймані, коледж природничих наук, кафедра фізики, вулиця Клясан, Сулейманія 46001, Регіон Курдистан, Ірак*

У цьому дослідженні розраховано гальмівну здатність позитронів у кількох біологічних тканинах в діапазоні енергій від 100 еВ до 1 МеВ. Основою методу є використання модифікованого виразу Бете-Блоха для гальмівної здатності та аналітичного виразу для ефективного атомного номера, включаючи ключові параметри, такі як середні енергії збудження атомів-мішеней, які суттєво впливають на результати гальмівної здатності. Аналітичні формули здебільшого використовувалися для розрахунку гальмівної здатності та діапазону CSDA з наближенням безперервного уповільнення. Розраховані результати гальмівної здатності та діапазону для позитронів у кількох сполуках, таких як тканини нирок, легень та щитовидної залози, порівнюються з результатами інших розрахунків, такими як програма Penelope 2012. Для розрахунків було використано моделювання методом Монте-Карло. Результати були представлені у вигляді графіків для демонстрації контрастів. Вони задовольняють визнану потребу медичної фізичної спільноти в даних про тканинно-специфічну взаємодію позитронів, що мають негайне застосування для покращення точності кількісного визначення зображень позитронно-емісійної томографії (ПЕТ) та уточнення дози опромінення для радіофармацевтичних препаратів, що випромінюють β-промені.

Ключові слова: *гальмівна здатність; позитрон; діапазон CSDA; енергія збудження; тканини людини*